

# Effects of molecular contamination and $sp^2$ carbon on oxidation of (100) single-crystal diamond surfaces

Ricardo Vidrio<sup>1,8,\*</sup>, Daniel Vincent<sup>2,8</sup>, Benjamin Bachman<sup>4</sup>, Cesar Saucedo<sup>4</sup>, Maryam Zahedian<sup>1</sup>, Zihong Xu<sup>1</sup>, Junyu Lai<sup>7</sup>, Timothy A. Grotjohn<sup>5</sup>, Shimon Kolkowitz<sup>6</sup>, Jung-Hun Seo<sup>7</sup>, Robert J. Hamers<sup>4</sup>, Keith G. Ray<sup>3</sup>, Zhenqiang Ma<sup>2</sup>, Jennifer T. Choy<sup>1,2,\*</sup>

<sup>1</sup>1500 Engineering Dr, Madison WI 53706, Department of Nuclear Engineering and Engineering Physics, University of Wisconsin-Madison

<sup>2</sup>1415 Engineering Dr, Madison WI 53706, Department of Electrical and Computer Engineering, University of Wisconsin-Madison

<sup>3</sup>7000 East Ave, Livermore CA 94550, Lawrence Livermore National Laboratory

<sup>4</sup>1101 University Ave, Madison WI 53706, Department of Chemistry, University of Wisconsin-Madison

<sup>5</sup>428 S Shaw Ln, East Lansing MI 48824, Electrical and Computer Engineering, Michigan State University

<sup>6</sup>1150 University Ave, Madison WI 53706, Department of Physics, University of Wisconsin-Madison

<sup>7</sup>135 Bell Hall, Buffalo NY 14260, Department of Materials Design and Innovation, University at Buffalo

<sup>8</sup>These authors contributed equally to this work.

---

## Abstract

The efficacy of oxygen (O) surface terminations of specific moieties and densities on diamond depends on factors such as crystallinity, roughness, and crystal orientation. Given the wide breadth of diamond-like materials and O-termination techniques, it can be difficult to discern which method would yield the highest and most consistent O coverage on a particular subset of diamond. We first review the relevant physical parameters for O-terminating single-crystalline diamond (SCD) surfaces and summarize prior oxidation work on (100) SCD. We then report on our experimental study on X-ray Photoelectron Spectroscopy (XPS) characterization of (100) diamond surfaces treated with oxidation methods that include wet chemical oxidation, photochemical oxidation with UV illumination, and steam oxidation using atomic layer deposition. We describe a rigorous XPS peak-fitting procedure for measuring the functionalization of O-terminated samples and recommend that the reporting of peak energy positions, line shapes, and full-width-half-maximum values of the individual components, along with the residuals, are important for evaluating the quality of the peak fit. Two chemical parameters on the surface,  $sp^2$  C and molecular contaminants, are also crucial towards interpreting the O coverage on the diamond surface and may account for the inconsistency in prior reported values in literature.

## 1. Introduction

Diamond is a material that is renowned for its unique properties such as extreme hardness [1] [2], high thermal conductivity [3], chemical inertness [4], and biocompatibility [5]. The surface science

\*Corresponding authors: [jennifer.choy@wisc.edu](mailto:jennifer.choy@wisc.edu) (Jennifer Choy)  
[vidrio@wisc.edu](mailto:vidrio@wisc.edu) (Ricardo Vidrio)

of diamond and diamond-like materials is an area of active research, as surfaces can be prepared with distinct surface chemistry for a wide range of applications, such as controlling the surface conductivity of diamond-based electronics [6] [7] [8], stabilizing near-surface color centers for quantum engineering uses [9] [10], and bio-sensing [11]. Given the breadth of uses for diamonds, researchers oftentimes turn to different forms of diamond for specialized applications. For example, nanodiamonds show promise towards becoming effective drug delivery systems [12] [13], while diamond thin films are necessary for incorporating diamond into electronic devices [14]. Given the variety of diamond-like materials, all with their own specially tailored applications, it can be difficult to filter the information necessary towards preparing an appropriate diamond surface to suit the individual needs of the researcher.

In this work, we describe and demonstrate experimental approaches to consistently prepare and interpret the results of oxidizing single crystalline diamond (SCD) surfaces cut in the (100) configuration. We begin with a discussion that identifies the most relevant physical parameters in oxidizing diamond, which include diamond type, surface cut, and roughness. This is followed by a compilation of prior oxidation results from literature, including summaries of the experimental methods, as well as the reported O(1s) atomic percentage values, from X-ray photoelectron spectroscopy (XPS). The experimental section consists of an explanation of the techniques we used to oxygen (O) terminate the diamond surface, including wet chemistry and dry oxidation methods, followed by a discussion of the materials characterization techniques, such as XPS and Atomic Force Microscopy (AFM), that were used to interpret the surface functionalizations.

We find that the presence of molecular contaminants on the diamond surface led to an exaggerated O atomic percentage and that an accumulation of  $sp^2$  C leads to a further increase in O(1s) content. Both these factors may account for the high variance in reported O(1s) atomic percentage values found in literature.  $sp^2$  C features prominently in all oxidized surfaces we studied and are further elevated by increased mechanical polishing, which is necessary for producing surface roughness below 1 nm. Based on our observations, we recommend a set of best practice approaches for preparing and characterizing oxidized diamond surfaces.

### 1.1 Factors that affect oxygen-termination behavior on single crystalline diamond

Different types of diamond today find their own respective uses in targeted applications. Some of the applications for SCDs include fabrication of low-loss power electronic devices [15] and vector

magnetometry via quantum sensing protocols [16]. Similar to other diamond-like surfaces, the surface chemistry of SCD can also be tailored for different applications. Although different types of surface terminations have been studied on diamond, including nitrogen [17], hydrogen [18], fluorine [19], and even silicon [20], O-terminations on diamond remains as some of the most widely adopted.

In particular, oxidized SCD surfaces play an important role in producing radiation detectors [21], generating high voltage diodes [22], and enhancing the stability of resonating nanostructures [23]. Here we group diamond oxidation methods into two different categories: wet or dry chemistry oxidation. As the name implies, wet chemistry oxidation (WCO) involves the use of acid solutions to induce O-termination on the diamond surface, while dry oxidation methods achieve O-termination with gases. Diamond oxidation behavior is influenced by a host of different factors, including crystallinity (single, poly-crystalline, nanocrystalline, etc.), diamond cut, and surface roughness.

#### *1.1.1 Crystallinity*

Klauser et. al compared the O content between hydrogen (H) terminated nanocrystalline and single crystalline diamond after exposure to wet and dry oxidation methods [24]. Between four different oxidation methods, including O plasma exposure, a sulfo-chromic acid bath, UV-ozone illumination, and an air-anneal, it was found that the nanocrystalline diamond (NCD) samples had at least twice the O content when compared to their SCD counterparts. The authors attributed this difference in O content due to the increased surface area present on the NCD surface. Similar results have been observed in other diamond-like oxidation studies, as Li et. al [25] who performed a multitude of wet chemistry treatments on polycrystalline diamond (PCD) and diamond powder (DP), with the highest reported values being 9.2% and 9.6% respectively. By comparison, the sulfo-chromic acid bath from Klauser et. al for both the (100) and (111) single crystalline surfaces reached a value of roughly 6.0 O(1s) at%.

#### *1.1.2 Crystal Orientation*

Another important factor in diamond oxidation behavior, particularly for SCD, is the type of surface orientation, usually available as (100), (110), and (111). Depending on the application towards which the diamond is being used, different orientations might have distinct advantages over other orientation types. For example, (111) diamond may be of interest in some quantum

information and sensing applications, since it is possible to produce nitrogen-vacancy (NV) centers along a single crystallographic axis [26] [27]. Furthermore, high-power electronics can also stand to benefit from the (111) diamond configuration, as this orientation is known to exhibit higher donor activity [28].

Regardless, (100) diamond remains as one of the most used orientations for several reasons. For one, growing (111) SCD through chemical vapor deposition (CVD) is difficult due to the onset of twinning and stacking faults that form on the (111) directions [29] [30] [31] [32]. Second, it proves challenging to grow (111) SCD thicker than 100 nm with low surface roughness [33] [34]. (111) diamond also has one of the lowest material removal rates when compared to both (100) and (110) diamond [35], meaning that attaining a lower surface roughness could prove more difficult.

The most notable difference between oxidizing (100) and (111) diamond is the preferred bonding configurations of O on the surface, based on ab initio density functional theory (DFT). Experimentally, Klauser et. al presented data on the bonding present on O plasma oxidized H-terminated single crystalline (100) and (111) diamond [24], and showed that when subjected to the same oxidation treatment, O contents for both diamond types were roughly equal. However, the XPS peak deconvolution revealed that the (111) diamonds had a higher percentage of carbonyl bonds, when compared to the (100) diamonds. The (100) diamonds also had a higher percentage of ether bonds when compared against the (111) diamonds, but ether bonds were still prominent on the (111) surface.

Another study yielded results that contradicted Klauser et. al, as Damle et. al had subjected (100), (111), and (110) diamond to a boiling  $\text{H}_2\text{SO}_4\text{:HNO}_3$  bath at 3:1 volumetric mixture for 4 hours at 140°C and had found differing amount of O(1s) percentages for all three diamond orientations [36]. The (100) diamond had an O atomic percentage of  $13.73 \pm 5.42\%$ , while the (111) diamond had  $15.12 \pm 0.85\%$ . In this case, these results contradict what was observed in Klauser et. al [24], as the (111) surface tended to exhibit the higher O content. In comparison to (100) and (111), the (110) surface had the lowest amount of O content, at  $10.09 \pm 2.57\%$ . Future work is needed to elucidate the reason behind these differing O amounts on different surfaces. Another study, Wang et. al, also looked at the difference between the amount of carboxylic acid groups present on both (100) and (111) single crystalline diamond surfaces, with a thin boron doped layer, after being subjected to H-termination and subsequent acid oxidation to induce carboxylation [37]. The study

found that this treatment yielded nearly twice the amount of carboxylic acid groups on the (100) surface when compared to (111). The authors reasoned that this was due to the presence of both  $S_A$  and  $S_B$  step edges on the (100) surface, the latter of which are more conducive towards harboring  $CH_3$  bonds, which prove essential toward carboxylation.

### *1.1.3 Surface Roughness*

Another factor that affects diamond oxidation is surface morphology, as a roughened surface has a higher likelihood of harboring inhomogeneities, such as different dips, cracks, or crevices which could lead to non-homogenous coverage of oxygen content. For example, Pehrsson et. al showed that H-terminated (100) SCD surfaces, smoothened by H plasma treatment, developed ether, carbonyl, and hydroxyl groups after exposure to thermally activated O gas [38]. The authors suggested that the initial oxidation proceeds on defect sites on the diamond, such as on steps or edges, and results in the formation of carbonyl and hydroxyl bonds. Afterwards, O will tend to bond in the ether formation in more smoothened low index sites, resulting in a predominantly ether bonded surface. Although a popular practice to smoothen the diamond surface is mechanical polishing, a molecular dynamics study by Zong et. al showed that mechanical polishing of the diamond crystal results in an increase in the presence of  $sp^2$  C [39]. The authors show that due to the onset of mechanical compression and scratching, the  $sp^3$  C diamond will transform to non-diamond phases consisting of amorphous  $sp^0$ ,  $sp^1$ ,  $sp^2$ , and  $sp^3$ , with the  $sp^2$  and amorphous  $sp^2$  C being the most predominant. This in turn could have ramifications for both the surface chemistry and bandgap energy of the diamond, as the presence of  $sp^2$  C changes the work function of the material [40].

## 1.2 Review of prior oxidation experimental methods on (100) single-crystalline diamond

The most common approach to quantify the extent of the O coverage on the SCD surface is to use XPS to determine the total percentage of O atoms, relative to C atoms, that are present on the surface. To put the O(1s) atomic % in context, using the NIST Effective-Electron-Attenuation Length Database [41], and assuming a terminal layer of  $sp^3$  C on diamond, we determine that the surface C atoms on (100) diamond contributes to 6.4% of the C XPS counts for a pristine sample. Both ether and carbonyl groups can form with surface C atoms on the diamond (100) surface at a 1:1 O:C ratio. Therefore, if the XPS counts come only from O(1s)-oxygen bound to the (100) diamond surface (in the form of surface  $C=O$  (carbonyl) and  $C-O$ (ether) groups) and C-C from  $sp^3$

diamond, then a monolayer coverage of oxygen would correspond to the sum of C=O and C-O counts, or equivalently the O(1s) counts, being 6.0% of the total XPS signal. Although the idea of a monolayer can be useful for visualizing how oxygen can bond to a surface composed of  $sp^3$  C, recent work points to the fact that diamond is multi-layered, with the most superficial layer consisting of most of the O content followed by  $sp^2$  C, and then the  $sp^3$  C diamond comprising the bulk of the material [42] [43]. Table 1 compiles the experimental methods and results for representative prior work on oxidation of (100) SCD samples.

*Table 1: Compilation of experimental oxidation methods and results that have been used on (100) single-crystalline diamond.*

Category of treatment	Oxidation Method	O1s At %	Reference
Wet	H <sub>2</sub> SO <sub>4</sub> :HNO <sub>3</sub> (3:1) for 4 hours at 140°C	13.73 ± 5.42	Damle et. al (2020) [36]
Wet	Hydrogen-termination, H <sub>2</sub> SO <sub>4</sub> :HNO <sub>3</sub> bath, NaOH bath, and HCl bath	16	Wang et. al (2011) [37]
Wet	Tri-acid clean/HClO <sub>4</sub> :H <sub>2</sub> SO <sub>4</sub> :HNO <sub>3</sub> (1:1:1) for 2 hours	8.5	Cui et. al (2013) [46]
Wet	Tri-acid Clean/HClO <sub>4</sub> :H <sub>2</sub> SO <sub>4</sub> :HNO <sub>3</sub> (1:1:1) for 1 hour	4.81 ± 0.78	Sangtawesin et. al (2019) [9]
Wet	Tri-acid clean/HClO <sub>4</sub> :H <sub>2</sub> SO <sub>4</sub> :HNO <sub>3</sub> (1:3:4) for 2 hours	4.94	Alba et. al (2020) [42]
Wet	H-termination, Sulfo-Chromic Acid at 230-250°C	6.8	Klauser et. al (2010) [24]
Dry	H-termination, O plasma	6.64	Klauser et. al (2010) [24]
Dry	H-termination, Thermal Oxidation at atmospheric conditions at 700 °C for 5 minutes	5.85	Klauser et. al (2010) [24]
Dry	UV-Ozone illumination with atmospheric conditions	5.27	Klauser et. al (2010) [24]
Wet and Dry	Tri-acid Clean/HClO <sub>4</sub> :H <sub>2</sub> SO <sub>4</sub> :HNO <sub>3</sub> (1:1:1) for 1 hour + oxygen anneal + piranha clean	6.17 ± 0.78	Sangtawesin et. al (2019) [9]

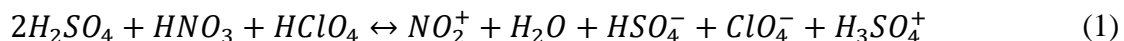
### *1.2.1 Wet Chemistry Oxidation (WCO) Treatments*

By far, the most prevalent of the oxidation methods reported has been exposure of diamond surfaces to aqueous mineral acids at elevated temperatures. WCO is also responsible for some of the highest oxygen atomic percentages reported in literature, up to 16% [37]. However, to our knowledge, there is no consensus on the mechanism responsible for diamond oxidation in literature; Li et. al proposed a mechanism and identified a possible oxidizing agent responsible for diamond oxidation based on their work with polycrystalline and diamond powders in  $\text{H}_2\text{SO}_4\text{:HNO}_3$  acid baths [25]. The authors explain that the reaction between  $\text{H}_2\text{SO}_4$  and  $\text{HNO}_3$  will result in  $\text{H}_2\text{NO}_3^+$  and  $\text{HSO}_4^-$ . The  $\text{H}_2\text{NO}_3^+$  will further decompose into  $\text{NO}_2^+$  and  $\text{H}_2\text{O}$ , while the  $\text{H}_2\text{O}$  will in turn become protonated, by  $\text{H}^+$ , which will result in the further production of  $\text{NO}_2^+$ . The authors go on to define that one of the main limitations of this mechanism is how the increase in  $\text{H}_2\text{SO}_4$  is unfavored in this constant-volume reaction, meaning that as the amount of  $\text{H}_2\text{SO}_4$  increases, the concentration of  $\text{NO}_2^+$  decreases. The authors identify this threshold ratio as 5:1, as anything past this only resulted in a reduced O atomic percentage on polycrystalline and diamond powder surfaces. Furthermore, the authors mention that this reaction is a temperature dependent process, as both reactants have markedly different boiling points, with  $\text{H}_2\text{SO}_4$  being at  $337^\circ\text{C}$  and  $\text{HNO}_3$  being at  $83^\circ\text{C}$ . As the temperature increases, this will cause a decrease in the presence of  $\text{HNO}_3$ , which in turn causes unfavorable conditions for oxygen-termination on the diamond surface. As evidence for this argument, the authors noted that the ratio of  $\text{H}_2\text{SO}_4\text{:HNO}_3$  that yielded the best O content decreased when the temperature of the experiment increased from  $195^\circ\text{C}$  to  $360^\circ\text{C}$ . Together, these two findings, led the authors to identify the main oxidizing species as  $\text{NO}_2^+$ , as this claim was also bolstered by how the presence of  $\text{NO}_2^+$  causes structural disorder on C structures [44].

As shown by Damle et. al [36], Wang et. al [37], and Maier et. al [45], a mixture of  $\text{H}_2\text{SO}_4$  and  $\text{HNO}_3$  acids are a commonly used and generally effective means of diamond surface oxidation. From these three studies, Damle et. al [42] reported XPS peak deconvolution results from the  $\text{C}(1s)$  spectra acquired through XPS. The authors had assigned peaks related to  $\text{sp}^2$  C,  $\text{sp}^3$  C, ethers, carbonyls, alcohols, and carboxylic acid groups. However, note that Wang et. al [37] relied on a H-termination, followed by the  $\text{H}_2\text{SO}_4\text{:HNO}_3$  clean, then a bath in 0.1 M of NaOH for two hours at  $90^\circ\text{C}$ , and followed by a bath in 0.1M of HCl for two hours at  $90^\circ\text{C}$ . The intent behind the H-termination was to help the conversion of dihydride and trihydride towards functionalized groups

on the diamond surface, which include carboxylic acid groups, polycarbonate bonds, and ester groups. The subsequent treatment of the NaOH will react with the ester groups to form sodium carboxylate. Exposing the sodium carboxylate to HCl will result in carboxyl acid as the terminal group, thus increasing the amount of carboxylic acid groups on the diamond surface. In fact, the authors had noted that this process led to a diverse functionalization on the surface, with ether, carbonyls, and carboxylic acid groups that were identified through peak deconvolution of the C(1s) spectra measured by XPS. This protocol had also resulted in the largest reported increase in O content of the (100) SCD surface, with as much as 16% oxygen.

Like the H<sub>2</sub>SO<sub>4</sub>:HNO<sub>3</sub> clean, the tri-acid clean relies on both H<sub>2</sub>SO<sub>4</sub> and HNO<sub>3</sub> for the oxidation process, but also includes HClO<sub>4</sub> in a 1:1:1 volumetric ratio between the other two acids. Cui et. al [46], Sangtawesin et. al [9], and Alba et. al [42] make mention of the oxygen atomic percentage from this technique, reporting it at 8.5%, 4.81 ± 0.78 %, and 4.94% respectively. Of these three, both Sangtawesin et. al [9] and Alba et. al [42] reported C(1s) XPS peak deconvolution info from their acid treatment results. Reported chemical groups following the tri-acid clean include sp<sup>3</sup> C, sp<sup>2</sup> C, ethers, and carbonyls [9] [42]. Although the tri-acid clean includes HClO<sub>4</sub>, the chemical reaction should proceed nearly identically to the H<sub>2</sub>SO<sub>4</sub>:HNO<sub>3</sub> clean, albeit with one more chemical species.



When compared to H<sub>2</sub>SO<sub>4</sub>:HNO<sub>3</sub>, the tri-acid mixture now includes the presence of two oxidizing agents, NO<sub>2</sub><sup>+</sup> and H<sub>3</sub>SO<sub>4</sub><sup>+</sup>, both of which could participate in the diamond oxidation process. Unlike the H<sub>2</sub>SO<sub>4</sub>:HNO<sub>3</sub> mixture, here the oxidizing potential is not limited by the increase in H<sub>2</sub>SO<sub>4</sub>, as increasing the amount of H<sub>2</sub>SO<sub>4</sub> will result in an increase of H<sub>3</sub>SO<sub>4</sub><sup>+</sup>, although this will come at the cost of decreasing the amount of NO<sub>2</sub><sup>+</sup>. As of the time of this writing, it is unclear whether the tri-acid clean could theoretically yield a higher O content as compared to the H<sub>2</sub>SO<sub>4</sub>:HNO<sub>3</sub> clean, since there is a lack of data as to whether the presence of both NO<sub>2</sub><sup>+</sup> and H<sub>3</sub>SO<sub>4</sub><sup>+</sup>, would lead to more oxidation, or alternatively, which of these species could prove the better oxidation agent between the two. Although the nitric-sulfuric mixtures are prolific in their use of diamond oxidation, there are other acids which have also been employed towards O-terminating diamond. Although sparse, these include sulfo-chromic acid [24], aqua regia [47], and



CrO<sub>3</sub>:H<sub>2</sub>SO<sub>4</sub> [48]. The results of subjecting the diamond surface to these acids are shown in Table 1.

### *1.2.2 Dry Oxidation Methods*

An alternative to liquid acids for oxidizing diamond surfaces includes exposure to O gases, often under photochemical (via UV exposure) or plasma discharge conditions, as shown in [24] and [49] in Table 1. Klauser et. al exposed (100) and (111) H-terminated SCD samples to an O plasma environment which resulted in an O atomic percentage of 6.64%, comparable to the sulfo-chromic method. The efficacy of this method relies on the direct adsorption of O on the diamond surface, as was demonstrated by Enriquez et. al [50]. In this study, the authors used density functional theory calculations to show the diamond oxidation mechanisms that occur from an oxygen plasma etching process. The authors found that at low surface coverages, the direct adsorption of oxygen on the diamond surface will cause severing of carbon dimer bonds and will result in energetically favorable carbonyl bonds. However, as the oxygen surface coverage increases, ether bonds will tend to be more stable than carbonyls, as an increase in oxygen coverage towards a full monolayer will tend to favor ether bonding.

Similarly, Klauser et. al utilized a series of different annealing temperatures with varying exposure times to achieve thermal oxidation with H-terminated diamond surfaces in air [24]. The increase in annealing temperature corresponded to the highest amount of O atomic percentage at 5.85%, while anything lower than this temperature only yielded lower oxygen percentages. Prior work has revealed that thermal oxidation is effective in producing O-terminated diamond surfaces, as John et. al observed ether and carbonyl groups after subjecting polycrystalline diamond films to 11-760 torr of dry O in temperatures at excess of 500°C [51]. A complete mechanism of thermal oxidation on diamond surfaces is still unclear as of the time of this writing, however work on H-terminated single crystalline (100) diamond surfaces, by Pehrsson et. al [52], revealed that, at temperatures below 950°C, minimal surface coverage of O is possible, due to reactions occurring at defect sites on the diamond. Past 950°C hydrogen directly desorbs from the diamond surface, resulting in higher amounts of O coverage and an overlayer of sp<sup>2</sup> C.

Finally, both Riedel et. al [49] and Klauser et. al [24] relied on an ozone treatment to achieve O-termination on (100) single crystalline diamond. In Riedel et. al treatment, the diamonds were first O-terminated by a H<sub>2</sub>SO<sub>4</sub>:HNO<sub>3</sub> boiling bath and subsequently H-terminated via plasma [49]. The

diamonds were then oxidized by a mixture of O<sub>2</sub> and O<sub>3</sub> emanating from a commercial ozone generator. O-termination was confirmed via XPS. Klauser et. al also utilized an ozone treatment for diamond oxidation, although in that study, ozone was formed via a UV-illumination process within a UV-ozone cleaner at room temperature [24]. Reaction mechanisms for ozone diamond oxidation are still unclear as of this time, but Speranza et. al has postulated six different mechanisms on hydrogenated polycrystalline diamond surfaces reacting with ozone [53]. All six mechanisms result in the formation of O<sub>2</sub> gas with the lowest activation energy out of these six reactions being the ether and carboxylic acid group.

Finally, Sangtawesin et. al [9] relied on a mixture of both wet and dry oxidation methods to achieve  $6.17 \pm 0.78$  % O content, comparable to what the authors term as a monolayer. Their technique relied on first tri-acid cleaning the diamond to start from an O-terminated surface. Afterward, the diamond was annealed in an O<sub>2</sub> chamber at 450°C for four hours. Subsequently, the diamond was piranha-cleaned for 20 minutes to remove any superficial forms of amorphous sp<sup>2</sup> C. C(1s) XPS peak deconvolution shows the presence of sp<sup>3</sup> C bonds, amorphous sp<sup>2</sup> C, carbonyls, and ethers.

## 2. Experimental Methods

### *2.1 Materials*

All diamonds used for this study are type IIa (100) SCD grown using CVD by Element 6. The type of diamonds employed here fall into two categories based on their surface roughness values as measured by AFM (Figure 1). As-received SCD samples from the vendor are typically polished to Ra < 30 nm as specified by the manufacturer (Figure 1a). We refer these samples as “regular-polished” diamonds. Diamonds that are referred to as “super-polished” have been mechanically polished to Ra < 1nm (Figure 1b) and underwent an Inductively Coupled Plasma – Reactive Ion Etching (ICP-RIE) process to remove any mechanical defects due to polishing [9]. The ICP-RIE consisted of 400 W of ICP power, 250 W substrate bias RF power, 25 sccm Ar, 40 sccm Cl<sub>2</sub>, 8 mTorr for 30 minutes which was then followed by 700 W ICP, 100 W substrate bias, 30 sccm O<sub>2</sub>, 10 mTorr for 25 minutes [9]. We estimate the etch depth to be roughly 3 microns. The regular-polished diamonds exhibit polishing marks from the manufacturers polishing, whereas the super-polished diamonds have a lack of these polishing marks due to the ICP-RIE.

## *2.2 Wet Chemistry Oxidation techniques*

All as-received diamonds were first tri-acid cleaned to remove superficial forms of  $sp^2$  from the CVD growth process or any forms of adventitious carbon. We investigated three wet oxidation approaches for this study: a tri-acid clean, an  $H_2SO_4:HNO_3$  bath, and a piranha clean. The tri-acid clean utilizes a Graham condenser and round bottom flask heater. The Graham condenser is required as a safety precaution to protect against the vapors of the boiling acid mixture, which holds steady at  $450^\circ C$ . Three acids,  $HClO_4$ ,  $H_2SO_4$ , and  $HNO_3$  are mixed in a 1:1:1 volumetric ratio. The acid mixture is then put in a 100 mL round bottom flask and the diamond sample is placed in the solution. The round bottom flask is then inserted to the Graham condenser and the mixture is allowed to sit and boil for one hour. The piranha clean procedure consists of first tri-acid cleaning the as-received diamonds to remove most organic contamination and residual  $sp^2$  carbon from the CVD growth process. Following the tri-acid clean, the diamonds are then submerged in a 3:1  $H_2SO_4:H_2O_2$  piranha clean mixture for five hours at  $110^\circ C$  [54]. Similarly, the  $H_2SO_4:HNO_3$  clean starts off by subjecting the as-received diamonds to a tri-acid clean. Afterwards, diamond samples were placed in a  $H_2SO_4:HNO_3$  bath in a 9:1 volumetric mixture at  $90^\circ C$  for 9 hours [55] [25].

## *2.3 H-termination and subsequent treatments*

Before H-termination took place, as-received diamond samples were first tri-acid cleaned to remove any contaminants and excess  $sp^2$  C from the CVD process. SCD samples were H-terminated by placing the diamonds within an  $H_2$  plasma chamber for roughly 15 minutes exposure. We then replicated the procedure by Wang et. al [37] to subject H-terminated diamond samples to first a  $H_2SO_4:HNO_3$  bath at  $90^\circ C$ , followed by a 0.1M bath of NaOH at  $90^\circ C$  for 2 hours, and then submerged in a 0.1M HCl bath at  $90^\circ C$  for 2 hours.

## *2.4 ALD and UV/Ozone treatments*

The atomic layer deposition (ALD) treatment utilized a Savannah S200 Series ALD System from Ultratech/Cambridge Nanotech. The process used a high-purity  $H_2O$  precursor to treat the surface over 15 (or 30 cycles) at a temperature of  $250^\circ C$ . Each cycle consisted of a 0.015s  $H_2O$  pulse followed by a 4s hold before purging the chamber. The UV/Ozone treatment was done using a Samco Model UV-1 UV Ozone Cleaner. The samples were processed at  $200^\circ C$ , while flowing 0.75L/min of oxygen, for 35 minutes.

## 2.5 Surface Characterization Techniques

Diamond samples underwent XPS analysis with a Thermo Scientific K-Alpha X-Ray Photoelectron Spectrometer. XPS protocol relied on collecting three different points on the surface with a 200- $\mu\text{m}$  spot size, culminating in at least six different survey results for each processing method. Furthermore, each spot measurement also collected narrow scans from the C1s and O1s regions. A 20-eV pass energy was chosen for all narrow scans, alongside a 0.1 eV step size. Peak fitting was performed on the C(1s) XPS data using CasaXPS analysis software [56]. A Bruker Icon Atomic Force Microscope was used to characterize the surface roughness and topology of diamond samples. AFM was employed to ascertain the difference between regular-polished and super-polished diamond samples. A comparison between the two types of surfaces is shown on Figure 1.

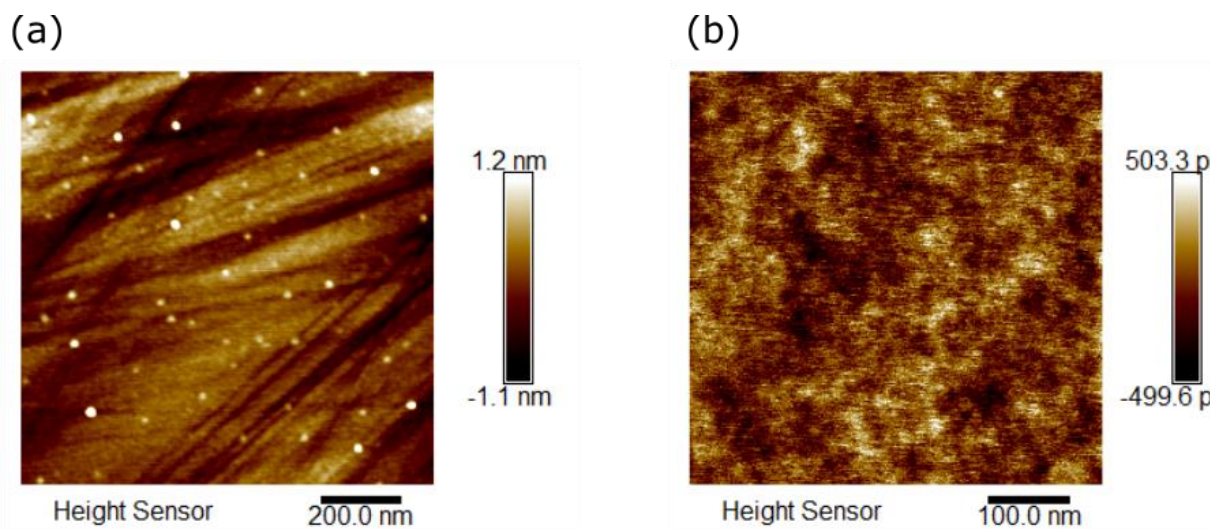


Figure 1: AFM results of (a) regular-polished (100) SCD surface and (b) super-polished (100) SCD surface.

## 3. Results and discussion

### 3.1 Impact of molecular contaminants on measured O concentration on the surface

Figure 2a shows the results of a representative survey spectra for a SCD surface. Visible peaks include the C(1s) and O(1s) regions, as well as their corresponding Auger peaks, labeled as CKLL and OKLL. Shown in the subset plot are some of the most common types of contaminants observed in the spectra which include the Si2s, Si2p, S2s, and S2p peaks. Not shown in the subplot is the N(1s) peak, which was also found during some measurements.

Of particular concern is how the O(1s) atomic percentage has a strong correlation with the amount of contaminants present on the sample. Figure 2b shows the relation between the sum of 2s and 2p atomic percentages for both silicon and sulfur, as a function of O(1s) atomic percentage for all three wet chemistry oxidation initial preparation methods. The amounts of the total silicon and sulfur contributions yield positive linear correlations with respect to the O(1s) atomic percentage.

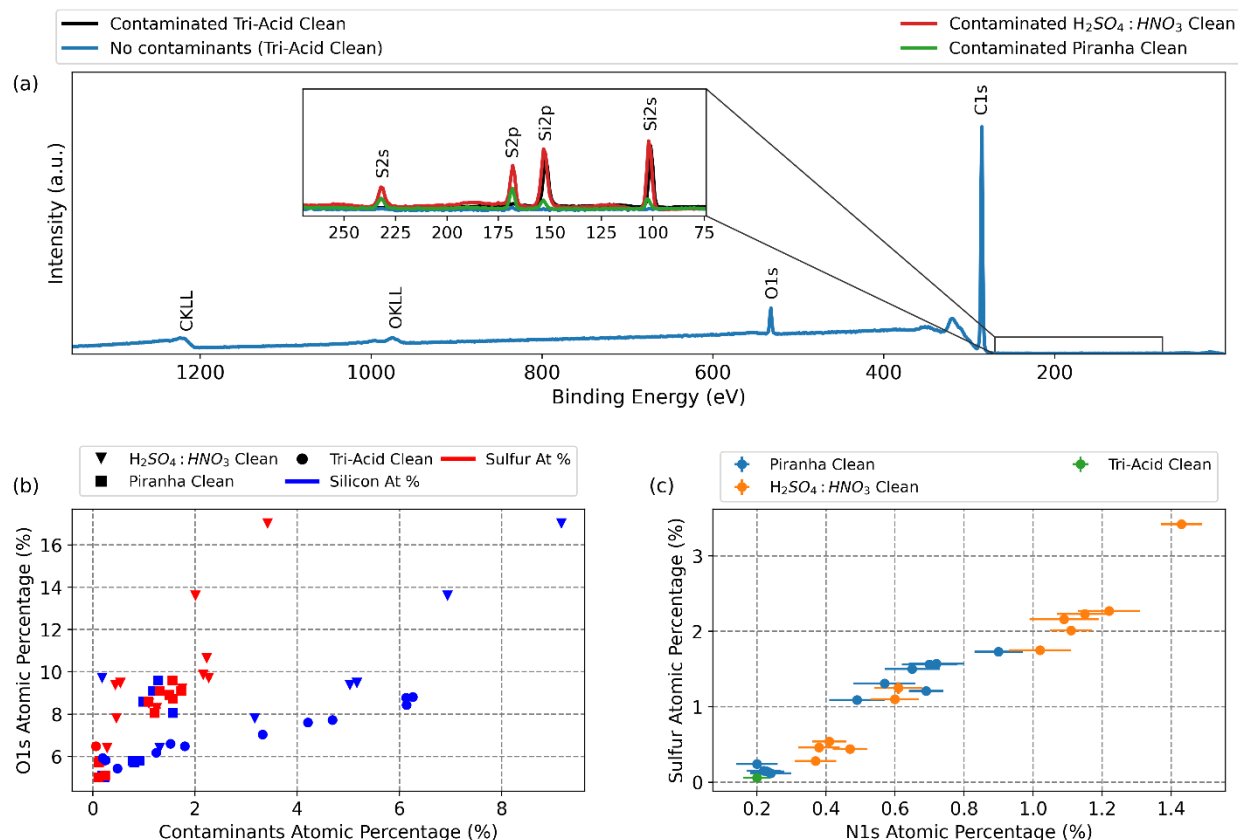


*Figure 2: (a) Representative survey plot for clean and contaminated diamond for three different WCO methods. (b) O(1s) plotted against the most prominent contaminants identified in the study, silicon and sulfur. The results from each WCO method are labeled accordingly. (c) The sum of the S(2s) and S(2p) contributions plotted against N(1s).*

We conclude that the presence of contaminants exaggerates the O content on the diamond surface. In other words, rather than the O(1s) signal coming from the O-terminated carbon on the SCD, the O(1s) signal includes the contribution from the contaminants and the functionalized surface.

It is believed that the Si(2s) and Si(2p) signals originate from either polydimethylsiloxane (PDMS), a contaminant that is ubiquitous on many surfaces in the everyday environment [57], or ambient SiO<sub>2</sub>. The S(2s) and S(2p) signals are believed to originate from ammonium sulphate, a contaminant that forms readily from any type of H<sub>2</sub>SO<sub>4</sub> acid clean, as the residual amount of

sulfuric acid on the diamond surface readily reacts to the nitrogen in the atmosphere, forming ammonium sulphate groups [58] [59]. The chemical origin of the individual contaminants is manifest in Figure 2b, as the slope for the sulfur at % is steeper than the silicon at %. This is due to how the O contribution from bonding to the sulfur atom is greater than its silicon counterpart.

Evidence of the presence of ammonium sulphate groups forming because of sulfuric acid cleans can be found in Figure 2c, as plotting the N(1s) atomic percentage versus the total sulfur atomic percentage, show a linear positive correlation, which indicates that the presence of any sulfur on the diamond surface is usually accompanied by nitrogen. We find that this corroborates the identity of ammonium sulphate groups, as such groups feature prominently on silicon surfaces following any type of clean involving sulfuric acid, such as the piranha clean.

To mitigate the effects of the contaminants, we improved the purity of the acids used for the treatments (by switching from laboratory grade to optima grade acids), stored diamond samples in polypropylene-based, cleanroom-grade containers (avoiding the use of gelpaks), and performed a thorough clean of the diamond surfaces using multiple rinses with deionized water and optima-grade isopropyl alcohol prior to drying surfaces. As a result of these practices, all subsequent wet chemistry oxidation results showed lower levels of contamination as compared to before. On average, the improved tri-acid clean has 0.10% of contamination observable on the diamond surface, while the sulphuric and piranha clean have 0.67% and 0.32% respectively.

### *3.2 Analysis of functionalizations on the SCD surface*

Figure 3(a) displays the C(1s) spectra, as well the peak-fitting results for a tri-acid cleaned regular-polished diamond sample. CasaXPS was utilized to perform all peak fits with C(1s) narrow scan spectra. A universal Tougaard baseline was used as the background for all C(1s) peak fits. Voigt functions, in the form of a Gaussian-Lorentzian product were applied for all fits. Although several authors make mention of constraining the FWHM for all C(1s) peak deconvolutions to about 1 eV [24] [60] [61], we find here that the residual STD is only minimized when the FWHM for the  $sp^3$  peak is roughly 0.6 eV and constrained within 0.6 to 0.7 eV. FWHM values for all other chemical

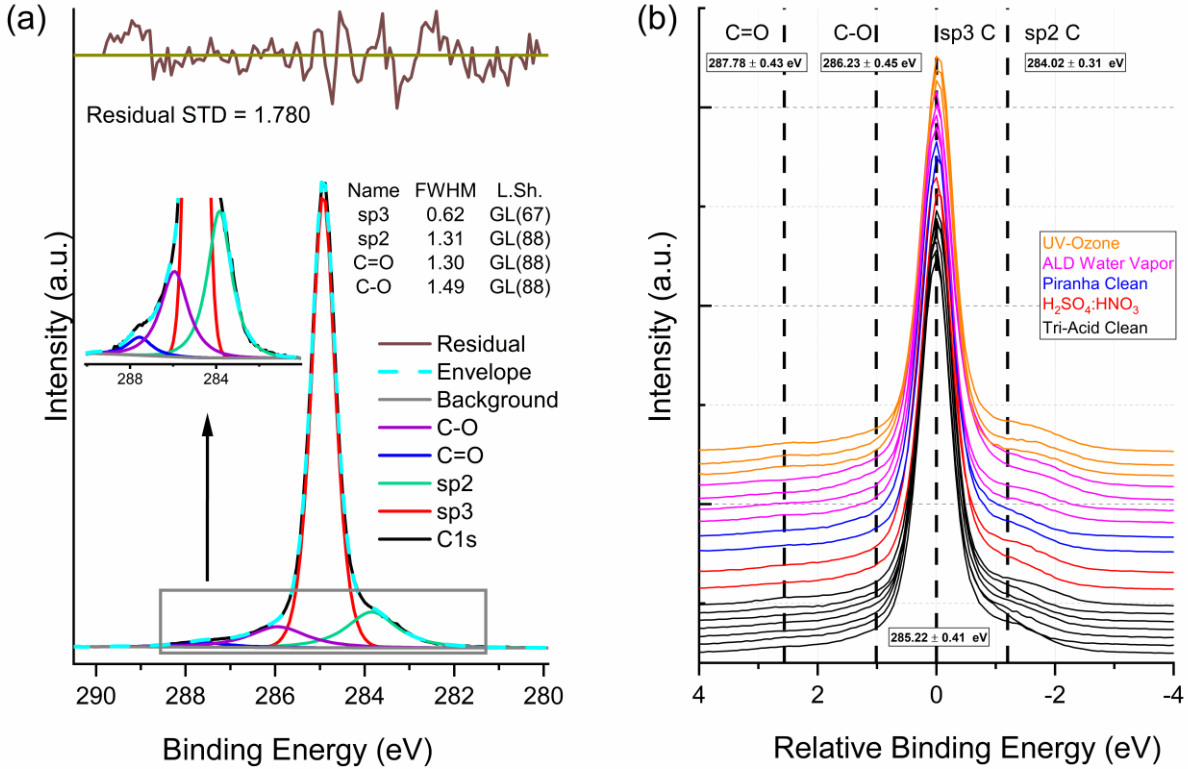


Figure 3: (a)  $C(1s)$  peak fitting results from CasaXPS displaying the individual chemical contributions, the FWHM values, and the line shape. (b) Overlaid plot of all  $C1s$  peaks, with their corresponding bond types and binding energy peak positions

species were constrained to within 1.30 to 1.6 eV. We ascertain that the lower FWHM for the  $sp^3$  C peak emanates from the bulk crystal structure and does not correspond to the shallowest layers of the diamond, which itself harbors only the  $sp^2$  C and oxygen contributions [42]. Furthermore, it is known that the FWHM for the  $sp^3$  diamond component is lower than the shallow topmost amorphous  $sp^2$  region [62].

Ideally, natural lineshapes emanating from XPS spectra should be Lorentzian, but Gaussian characteristics are introduced due to heterogeneity present in the sample [63] [64]. In this case, we find that the heterogenous nature of the diamond, i.e. a shallow amorphous  $sp^2$  C component followed by the bulk  $sp^3$  C diamond, introduces lineshapes of mixed Gaussian and Lorentzian character. These lineshapes take the form of a Gaussian – Lorentzian product function, labeled in Figure 3 and Figure 4 as GL. Seeing as how the functional groups are confined to only the uppermost portions of the diamond, we imposed identical FWHM constraints and Gaussian quality

on all the functional groups and  $sp^2$ , while giving the  $sp^3$  peak its own set of FWHM constraints and Gaussian character.

To generate chemically accurate C(1s) peak fits for all oxidized diamond data, peak positions and identities for the four chemical species labeled in Figure 3(a) were taken from established literature values [25] [9] [46]. While a multitude of C(1s) plots were analyzed, Figure 3(a) is representative of all SCD O-terminated peak fits analyzed in this study. Figure 3(b) shows the C(1s) spectra taken for all oxygen-treatments on SCD, plotted in terms of relative BE. Also shown in Figure 3(b) is the average and STD of the BE peak positions for all chemical components. The individual peak area contributions for all O-terminated diamonds for each of the chemical moieties can be found in the supplementary section of this text.

To emphasize, we note that to produce both physically meaningful and chemically accurate C(1s) peak fits representative of the functionalizations on the diamond surface it is vital to first constrain the appropriate fitting parameters, such as the FWHM, peak positions, and lineshapes. Once these constraints are applied to the model, only then does it become appropriate to attempt to fit the data such that the goodness-of-fit metric, in this case the residual STD, reaches a global minimum [64]. For a more in-depth analysis involved in the process of C(1s) peak fitting the reader is referred to other texts [57] [65] [64] [66] [67].

Despite the diamond being subjected to various wet chemistry oxidation methods, we still find that the  $sp^2$  content persists in all samples. In fact, this observation is consistent with prior work observed with SCD samples [9], PCD [25], and microcrystalline diamond (MCD) [43]. In Cobb et. al, it was shown that, despite applying a  $H_2SO_4:KNO_3$  clean to MCD, a layer of graphitic amorphous C remained on the surface, as verified through Scanning Transmission Electron Microscopy (STEM) [43]. Similarly, Li et. al showed that varying volumetric mixtures of  $H_2SO_4:HNO_3$  cleans and a piranha clean led to graphitic content on PCD surfaces as verified through XPS C(1s) peak deconvolution, with the piranha clean and aqua regia solution yielding the most graphite [25].

Given the ubiquitous presence of  $sp^2$  C on the diamond following all oxidation techniques, an H-termination was employed before subjecting the diamond to further oxidative treatment. Figure 4 displays the C(1s) spectra as well as the C(1s) peak deconvolution results for the H-termination and H-termination plus carboxylation (HPC) samples. Peak identities and positions for fitting the



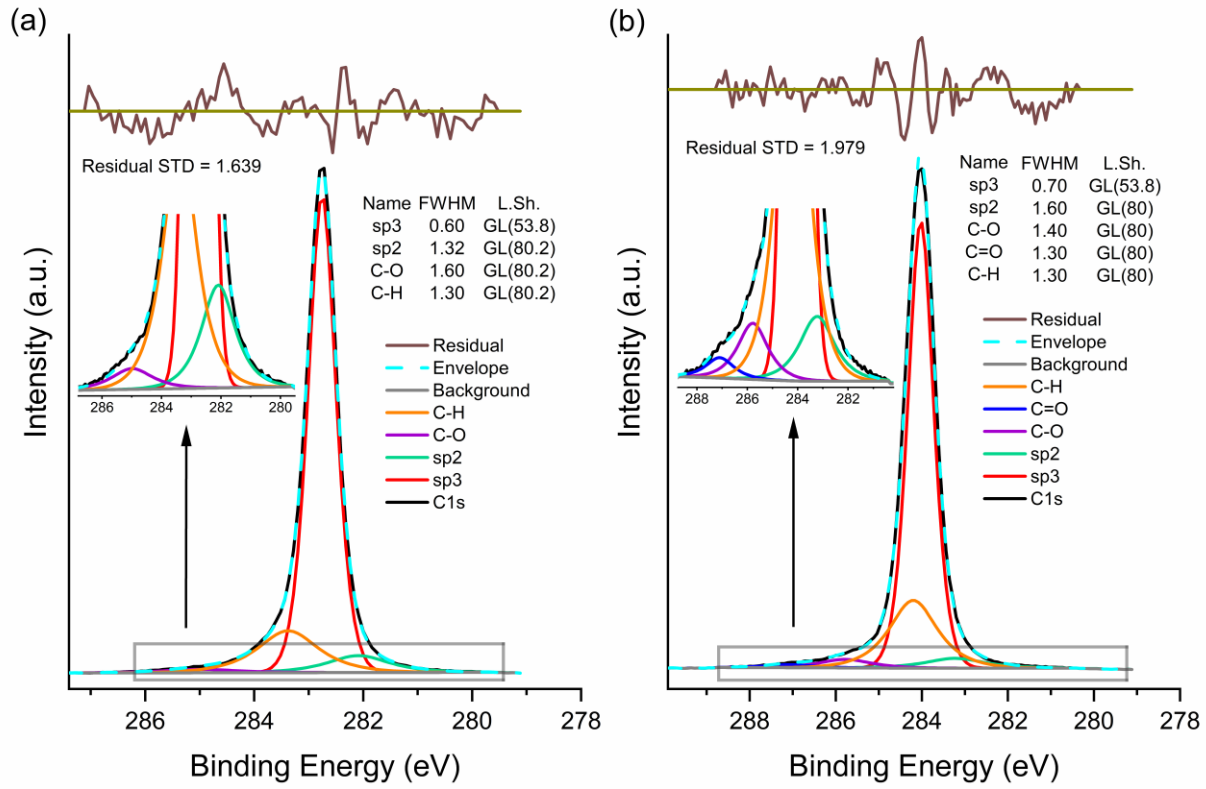


Figure 4: (a) Peak-fitting results and information for hydrogen terminated data (b) Peak-fitting results and information from hydrogen-termination plus carboxylation C1s peak.

H-terminations result shown in Figure 4a stem from Haensel et. al [68] and Paprocki et. al [69], while similar peak data for the HPC samples, shown in Figure 4b, come from Hoffman et. al [70], Ghodbane et. al (2010) [71], Ghodbane et. al (2006) [72]. The H-terminated data revealed only the presence of  $sp^3$  C, C-H, ethers, and a lowered presence of  $sp^2$  C. Whereas before in Figure 3a, the  $sp^2$  C peak accounted for  $13.75 \pm 0.17\%$  of the total area, in Figure 4a the  $sp^2$  C peak is now only  $6.40 \pm 0.23\%$ . The H-terminated plus carboxylation data reveals the presence of  $sp^3$  C,  $sp^2$  C, C-H, ether, and carbonyl bonds, with the  $sp^3$  C and C-H bonds being the most predominant.

We also note the presence of peak shifting from both sets of experiments in Figure 4 which can be explained by the C-H bonds on the diamonds surface. The H-bonds contribute to upward band bending which is caused by surface Fermi level pinning, which in turn reduces the barrier needed for electron emission from the  $sp^3$  C peak [73] [74]. As a result, we see that the  $sp^3$  C peak is lower in BE value for all H treated samples, with the effects being the most noticeable for the H-terminated samples as the  $sp^3$  peak position was  $282.77 \pm 0.0183$  eV when compared to the 285.22

$\pm 0.41$  eV measured from O-terminated samples. The H-terminated plus oxidation treated samples also displayed lower  $sp^3$  C peak position values at  $284.19 \pm 0.16$  eV, however the presence of oxygen bonds on the surface reduced the upward band bending effects.

The subsequent acid treatment, post H-termination, led to the rise of more surface functionalizations on the diamond, namely ether and carbonyls. However, note in Figure 4b that the C-H peak remains dominant when compared to the other peaks, and is  $21.39 \pm 0.67\%$  of the deconvoluted peak area. While the acid treatment has resulted in generating O functional groups, it was not successful in removing all the C-H bonds from the surface. This leads us to believe that the HPC method results in a partially functionalized surface, which is also evident by the increase in O1s at% between the H-terminated samples and HPC sample, as the change is  $2.12 \pm 0.72$  and  $3.47 \pm 0.37$  respectively. Finally, we find that the lowest amount of  $sp^2$  C peak area percentage, at  $3.83 \pm 0.48\%$ , was found for the HPC method which we attribute to an effective H-terminated surface, given that the majority of the surface was C-H bonds.

### *3.3 Relationship between O1s counts and the $sp^2$ content*

Figure 5 displays the relation between the  $sp^2$  C content of the diamond and the O(1s) narrow peak scan area. Note the presence of two different regions on Figure 5, which are readily identified by being either regular-polished or super-polished. The super-polished samples exhibit a higher amount of both  $sp^2$  C and O(1s) area counts, whereas the regular-polished samples are confined on the lower left-hand corner of the plot and feature lower  $sp^2$  C and O(1s) counts.

We find that the  $sp^2$  C contribution in the super-polished samples are greater due to the effects of the mechanical polishing, as computational simulations show that an accumulation of  $sp^2$  C is expected on the diamond surface with an increase in polishing time [39]. Furthermore, as shown by Alba et. al, an increase in the oxygen content on the diamond surface is accompanied by a net increase in the  $sp^2$  C contribution [42]. By using angle resolved XPS, Alba et. al was able to show the O(1s) atomic percentage as a function of single-crystalline depth and how the  $sp^2$  content of the C(1s) spectra varies with respect to depth. These results revealed that as the penetration depth of the XPS beam becomes shallower, the  $sp^2$  C will tend to increase. In doing so, the O content on the diamond also increases. The implications from Alba et. al suggest that the majority of the oxygen bonding takes place on the shallow  $sp^2$  C sites, rather than on the  $sp^3$  bonded C present in the bulk diamond. From the results in Figure 5 we find that the mechanical polishing contributed

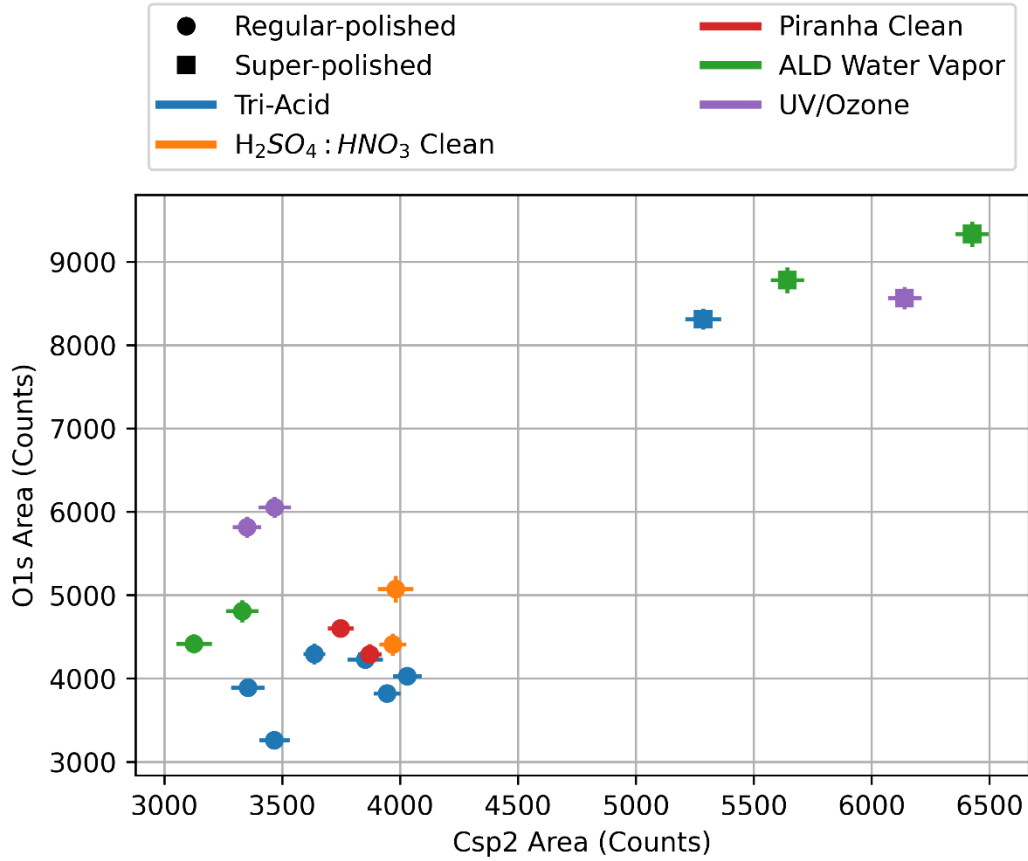


Figure 5:  $sp^2$  area plotted against  $O(1s)$  area measured for all wet chemistry and dry oxidation methods.

to a higher  $sp^2$  C content in the super-polished samples, which in turn resulted in a higher O content.

Given the results from both Alba et. al [42] and Zong et. al [39], we hypothesize that the conclusions from Figure 5 are a result of O-terminating diamond with differing amounts of  $sp^2$  C, introduced through the process of mechanical polishing. The mechanical polishing on the super-polished samples led to an increase of  $sp^2$  C which in turn is known to harbor a higher oxygen content. The regular-polished samples had a lower  $sp^2$  C and therefore a lower O contribution.

#### *Compilation of oxygen content from all surface treatments on single crystalline diamond*

Finally, the O-content results are summarized in Figure 6. Seeing as how the O atomic percentage displays a dependence with respect to the molecular contaminants and the  $sp^2$  C on the diamond surface, Figure 6 comes included with the contaminant atomic percentage and the  $sp^2$  C peak area counts, taken from the narrow scan C(1s) spectra peak-fitting results. The most right-hand side of

Figure 6 also includes the number of samples used for each treatment which is denoted as “N”. The contaminant atomic percentage is taken to be the total sum of the individual atomic percentage of the Si(2s), Si(2p), S(2s), S(2p), and N(1s) contributions. Given Figure 6 we identify the tri-acid clean as the cleanest WCO technique to O-terminate diamond, given that it has the lowest contaminant presence and the most repeatable O(1s) atomic percentage value, evidenced by the scale of its error bar when compared to the other methods. Despite the highest reported O atomic percentage being 16%, via the carboxylation method presented by Wang et. al [37], we were unable to replicate the results, and instead attained an oxygen atomic percentage of  $3.47 \pm 0.37\%$ .

As elaborated upon in the prior section, the super-polished samples all show exaggerated amounts of both  $sp^2$  C and O1s at%, with their regular-polished counterparts showing lower amounts of both species. Finally, we highlight both the ALD water vapor and UV/Ozone techniques as being comparatively effective at oxidizing diamond surfaces, with the data from regular-polished

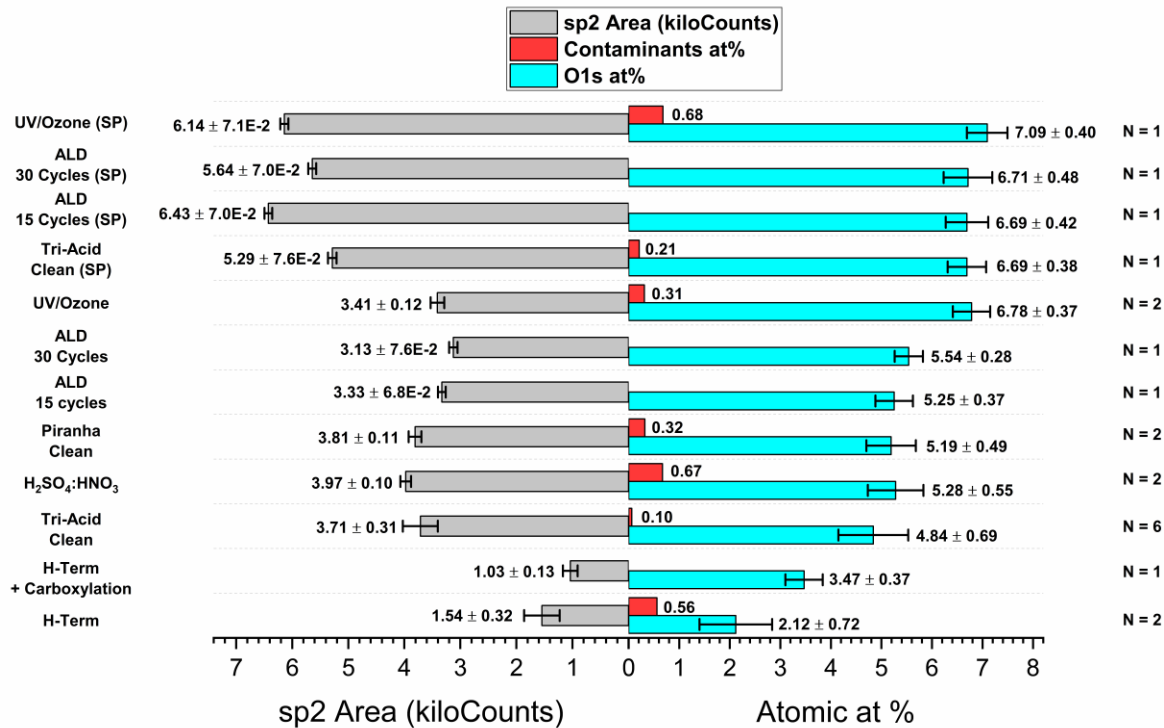


Figure 6: Bar plot with all diamond treatment methods showing the O1s atomic percentage, Contaminant atomic percentage, and the Csp2 content that was present on the diamond samples from XPS measurement. The right-hand side with the value of N shows the number of samples that were used for each treatment.

diamonds showing O1s at% values in excess of 5.25% with the ALD process resulting in some of the most contaminant-free surfaces studied for this work.

#### 4. Conclusion

In summary, we have compiled the appropriate sources of diamond oxidation from literature and summarized the information that is relevant only towards inducing effective O-termination on (100) SCD. While some of the most prominent methods for oxidizing diamond has been using wet chemistry (Table 1), the reported O atomic percentage values on the (100) single-crystalline diamond have a large variance, pointing to other factors that affect both the effectiveness of oxidation and the measured O content. We identify the two important parameters that complicate the observed O atomic percentage on the (100) SCD surface as the molecular contaminants and the  $sp^2$  content. We observe that both values have a dependence with respect to either the O atomic percentage or the raw O(1s) counts and thus encourage future work of SCD oxidation results to comment on the contaminant and the  $sp^2$  C amount visible on the surface.

Between the tri-acid clean,  $H_2SO_4:HNO_3$  clean, and the piranha clean, we identify the tri-acid clean as the WCO method as being the most viable for consistent and reproducible oxygen amount, as it yielded the lowest spread in oxygen atomic percentage and the cleanest surface. Dry oxidation methods, such as the photochemical oxidation via UV-illumination, and steam oxidation using ALD, are promising techniques that produce highest oxygen atomic percentages measured in this study. However, in combination with further mechanical polishing of the surface, these techniques also led to elevation in  $sp^2$  C content.

Finally, recent work points to the fact that SCD consists of layered regions comprised of different allotropes of carbon, with the topmost layer composed mostly of  $sp^2$  C and the bottommost layer being  $sp^3$  C. In this work, we introduced diamond samples with higher amounts of  $sp^2$  C as a consequence of mechanical polishing, which in turn led to more  $sp^2$  C sites and, subsequently, a higher O(1s) contribution. This effect was less prominent in the regular-polished samples, and as a result, we observe two different regions of surface O content for the diamond surface. Future experimental work should identify a technique that can correlate the thickness of the  $sp^2$  C on the SCD surface with the O(1s) content. Finally, we believe that the diamond community would benefit from an involved computational study that studies the effects of  $sp^2$  C content on electron

affinity, electronic bandgap, and oxygen coverage, as prior computational studies have only considered a  $sp^3$  C surface without any  $sp^2$  C bonding sites.

### Acknowledgements

This work is supported by the U.S. Department of Energy, Office of Science, Basic Energy Sciences under Award #DE-SC0020313. Part of this work was performed under the auspices of the U.S. Department of Energy at Lawrence Livermore National Laboratory under Contract DE-AC52-07NA27344. Contributions by Robert J. Hamers, Cesar Saucedo, and Benjamin Bachman were supported by NSF CHE-1839174. The authors gratefully acknowledge use of facilities and instrumentation supported by NSF through the University of Wisconsin Materials Research Science and Engineering Center (DMR-1720415).

### References

- [1] N. Novikov and S. Dub, "Hardness and fracture toughness of CVD diamond film," *Diamond and Related Materials*, vol. 5, no. 9, pp. 1026-1030, 1996.
- [2] C. Brookes and E. Brookes, "Diamond in perspective: a review of mechanical properties of natural diamond," *Diamond in perspective: a review of mechanical properties of natural diamond*, vol. 1, no. 1, pp. 13-17, 1991.
- [3] D. Twitchen, C. Pickles, S. Coe, R. Sussmann and C. Hall, "Thermal conductivity measurements on CVD diamond," *Diamond and Related Materials*, vol. 10, no. 3-7, pp. 731-735, 2001.
- [4] A. Grill, "Diamond-like carbon coatings as biocompatible materials - an overview," *Diamond and Related Materials*, vol. 12, no. 2, pp. 166-170, 2003.
- [5] L. Tang, C. Tsai, W. Gerberich, L. Kruckeberg and D. Kania, "Biocompatibility of chemical-vapour-deposited diamond," *Biomaterials*, vol. 16, no. 6, pp. 483-188, 1995.
- [6] A. Hokazono, K. Tsugawa, H. Umezana, K. Kitatani and H. Kwarada, "Surface p-channel metal-oxide-semiconductor field effect transistors fabricated on hydrogen terminated (001) surfaces of diamond," *Solid-State Electronics*, vol. 43, no. 8, pp. 1465-1471, 1999.
- [7] H. Karawada, "High-Current Metal Oxide Semiconductor Field-Effect Transistors on H-terminated Diamond surfaces and their High-Frequency Operation," *Japanese Journal of Applied Physics*, vol. 51, no. 9R, p. 090111, 2012.
- [8] Z. Yin, M. Tordjman, A. Vardi, R. Kalish and J. A. del Alamo, "A Diamond:H/WO<sub>3</sub> Metal-Oxide-Semiconductor Field-Effect Transistor," *IEEE Electron Device Letters*, vol. 39, no. 4, pp. 540-543, 2018.

- [9] S. Sangtawesin, B. L. Dwyer, S. Srinivasan, J. J. Allred, L. V. Rodgers, K. De Greve, A. Stacey, N. Donschuk, K. M. O'Donnell, D. Hu, D. A. Evans, C. Jaye, D. A. Fischer, M. L. Markham, D. J. Twitchen, H. Park, M. D. Lukin and N. P. de Leon, "Origins of Diamond Surface Noise Probed by Correlating Single-Spin Measurements with Surface Spectroscopy," *Physical Review X*, vol. 9, no. 3, p. 031052, 2019.
- [10] F. F. de Oliveira, S. A. Momenzadeh, Y. Wang, M. Konuma, M. Markham, A. M. Edmonds, A. Denisenko and J. Wrachtrup, "Effect of low-damage inductively coupled plasma on shallow nitrogen-vacancy centers in diamond," *Applied Physics Letters*, vol. 107, no. 7, p. 073107, 2015.
- [11] S. Wenmackers, V. Varmeren, M. vandeVen, M. Ameloot, N. Bijmens, K. Haenen, L. Michiels and P. Wagner, "Diamond-Based DNA sensors: surface functionalization and read-out strategies," *physica status solidi (a)*, vol. 206, no. 3, pp. 391-408, 2009.
- [12] G. Xi MD, PhD, E. Robinson PhD, B. Mania-Farnell PhD, E. Fausto Vanin PhD, K.-W. Shim MD, PhD, T. Takao MD, PhD, E. Victoria Allender MS, C. Shekhar Mayanil PhD, M. Bento Soares PhD, D. Ho PhD and T. Tomita MD, "Convection-enhanced delivery of nanodiamond drug delivery platforms for intracranial tumor treatment," *Nanomedicine; Nanotechnology, Biology, and Medicine*, vol. 10, no. 2, pp. 381-391, 2014.
- [13] X.-Q. Zhang, R. Lam, X. Xu, E. K. Chow, H.-J. Kim and D. Ho, "Multimodal Nanodiamond Drug Delivery Carriers for Selective Targeting, Imaging, and Enhanced Chemotherapeutic Efficacy," *Advanced materials*, vol. 23, no. 41, pp. 4770-4775, 2011.
- [14] A. T. Collins, "Diamond electronic devices - a critical appraisal," *Semiconductor science and technology*, vol. 4, no. 8, p. 605, 1989.
- [15] S. Shikata, "Single crystal diamond wafers for high power electronics," *Diamond and Related Materials*, vol. 65, pp. 168-175, 2016.
- [16] J.-P. Tetienne, N. Donschuk, D. A. Broadway, A. Stacey, D. A. Simpson and L. C. Hollenberg, "Quantum Imaging of current flow in graphene," *Science Advances*, vol. 3, no. 4, p. e1602429, 2017.
- [17] M. Attrash, M. K. Kuntumalla, S. Michaelson and A. Hoffman, "Nitrogen terminated diamond (111) by RF(N<sub>2</sub>) plasma - chemical states, thermal stability, and structural properties," *Surface Science*, vol. 703, p. 121741, 2021.
- [18] B. D. Thoms, M. S. Owens, J. E. Butler and C. Spiro, "Production and characterization of smooth, hydrogen-terminated diamond C(100)," *Applied Physics Letters*, vol. 65, no. 23, p. 1994, Applied Physics Letters.
- [19] K. Rietwyk, S. Wong, L. Cao, K. O'Donnell, L. Ley, A. Wee and C. Pakes, "Work function and electron affinity of the fluorine-terminated (100) diamond surface," *Applied Physics Letters*, vol. 102, no. 9, p. 091604, 2013.

- [20] A. Schenk, A. Tadich, M. Sear, K. M. O'Donnell, L. Ley, A. Stacey and C. Pakes, "Formation of a silicon terminated (100) diamond surface," *Applied Physics Letters*, vol. 106, no. 19, p. 191603, 2015.
- [21] K. Su, Z. Ren, J. Zhang, L. Liu, J. Zhang, Y. Zhang, Q. He, C. Zhang, X. Ouyang and Y. Hao, "High performance hydrogen/oxygen terminated CVD single crystal diamond radiation detector," *Applied Physics Letters*, vol. 116, no. 9, p. 092104, 2020.
- [22] D. Twitchen, A. Whitehead, S. Coe, J. Isberg, J. Hammersberg, T. Wikström and E. Johansson, "High-Voltage Single-Crystal Diamond Diodes," *IEEE Transactions on electron devices*, vol. 51, no. 5, pp. 826-828, 2004.
- [23] Y. Tao, J. Boss, B. Moores and C. Degen, "Single-crystal diamond nanomechanical resonators with quality factors exceeding one million," *Nature communications*, vol. 5, no. 1, pp. 1-8, 2014.
- [24] F. Klauser, S. Ghodbane, R. Boukherroub, S. Szunerits, D. Steinmüller-Nethl, E. Bertel and N. Memmel, "Comparison of different oxidation techniques on single-crystal and nanocrystalline diamond surfaces," *Diamond and Related Materials*, vol. 19, no. 5-6, pp. 474-478, 2010.
- [25] C. Li, X. Zhang, E. F. Oliveira, A. B. Puthirath, M. R. Neupane, J. D. Weil, A. Glen Birdwell, T. G. Ivanov, S. Kong, T. Gray, H. Kannan, A. Biswas, R. Vajtai, D. S. Galvao and P. M. Ajayan, "Systematic comparison of various oxidation treatments on diamond surface," *Carbon*, vol. 182, pp. 725-734, 2021.
- [26] J. Michl, T. Teraji, S. Zaiser, I. Jakobi, G. Waldherr, F. Dolde, P. Neumann, M. W. Doherty, N. B. Manson, J. Isoya and J. Wrachtrup, "Perfect alignment and preferential orientation of nitrogen-vacancy centers during chemical vapor deposition diamond growth on (111) surfaces," *Applied Physics Letters*, vol. 104, no. 10, p. 102407, 2014.
- [27] H. Ishiwata, M. Nakajima, K. Tahara, H. Ozawa, T. Iwasaki and M. Hatano, "Perfectly aligned shallow ensemble nitrogen-vacancy centers in (111) diamond," *Applied Physics Letters*, vol. 111, no. 4, p. 043103, 2017.
- [28] A. Tallaire, J. Achard, A. Boussadi, O. Brinza, A. Gicquel, I. Kupriyanov, Y. Palyanov, G. Sakr and J. Barjon, "High quality thick CVD diamond films homoepitaxially grown on (111)-oriented substrates," *Diamond and Related Materials*, vol. 41, pp. 34-40, 2014.
- [29] C.-S. Yan and Y. K. Vohra, "Multiple twinning and nitrogen defect center in chemical vapor deposited homoepitaxial diamond," *Diamond and Related Materials*, vol. 8, no. 11, pp. 2022-2031, 1999.
- [30] M. Kasu, T. Makimoto, W. Ebert and E. Kohn, "Formation of stacking faults containing microtwins in (111) chemical-vapor-deposited diamond homoepitaxial layers," *Applied Physics Letters*, vol. 83, no. 17, pp. 3465-3467, 2003.



- [31] I. Sakaguchi, M. Nishitani-Gamo, K. P. Loh, H. Haneda and T. Ando, "Homoepitaxial growth and hydrogen incorporation on the chemical vapor deposited (111) diamond," *Journal of applied physics*, vol. 86, no. 3, pp. 1306-1310, 1999.
- [32] M. Kasu, T. Makimoto, W. Ebert and E. Kohn, "Formation of stacking faults containing microtwins in (111) chemical-vapor-deposited diamond homoepitaxial layers," *Applied Physics Letters*, vol. 83, no. 17, pp. 3465-3467, 2003.
- [33] S. M. Parks, R. R. Grote, D. A. Hopper and L. C. Bassett, "Fabrication of (111)-faced single-crystal diamond plates by laser nucleated cleaving," *Diamond and Related Materials*, vol. 84, pp. 20-25, 2018.
- [34] C. Widmann, M. Hetzl, S. Drieschner and C. Nebel, "Homoepitaxial growth of high quality (111)-oriented single crystalline diamond," *Diamond and Related Materials*, vol. 72, pp. 41-46, 2017.
- [35] H. Luo, K. M. Ajmal, W. Liu, K. Yamamura and H. Deng, "Polishing and planarization of single crystal diamonds: state-of-the-art and perspectives," *Journal of Extreme Manufacturing*, vol. 3, no. 2, p. 02203, 2021.
- [36] V. Damle, K. Wu, O. De Luca, N. Orti-Casan, N. Norouzi, A. Morita, J. de Vries, H. Kaper, I. S. Zuhorn, U. Eisel, D. E. Vanpoucke, P. Rudolf and R. Schirhagl, "Influence of diamond crystal orientation on the interaction with biological matter," *Carbon*, vol. 162, pp. 1-12, 2020.
- [37] X. Wang, A. R. Ruslinda, Y. Ishiyama, Y. Ishii and H. Kawarada, "Higher coverage of carboxylic acid groups on oxidized single crystal diamond (001)," *Diamond and related materials*, vol. 20, no. 10, pp. 1319-1324, 2011.
- [38] P. E. Pehrsson and T. Mercer, "Oxidation of the hydrogenated diamond (100) surface," *Surface science*, vol. 460, no. 1-3, pp. 49-66, 2000.
- [39] W. Zong, X. Cheng and J. Zhang, "Atomistic origins of material removal rate anisotropy in mechanical polishing of diamond crystal," *Carbon*, vol. 99, pp. 186-194, 2016.
- [40] K. Akada, S. Obata and K. Saiki, "Work Function Lowering of Graphite by Sequential Surface Modifications: Nitrogen and Hydrogen Plasma Treatment," *ACS omega*, vol. 4, no. 15, pp. 16531-16535, 2019.
- [41] C. Powell and A. Jablonski, "NIST Electron Effective-Absorption-Length Database Version 1.3," National Institute of Standards and Technology, Gaithersburg, 2011.
- [42] G. Alba, M. Pilar Villar, R. Alcantara, J. Navas and D. Araujo, "Surface States of (100) O-Terminated Diamond: Towards Other 1x1:O Reconstruction Models," *Nanomaterials*, vol. 10, no. 6, p. 1193, 2020.
- [43] S. J. Cobb, F. H. Laidlaw, G. West, G. Wood, M. E. Newton, R. Beanland and J. V. Macpherson, "Assesment of acid and thermal oxidation treatments for removing sp<sup>2</sup>

- bonded carbon from the surface of boron doped diamond," *Carbon*, vol. 167, pp. 1-10, 2020.
- [44] A. B. Porto, G. G. Silva, H. F. dos Santos and L. F. de Oliveira, "Oxidation of Single-Walled Carbon Nanotubes under Controlled Chemical Conditions," *Journal of the Brazilian Chemical Society*, vol. 29, pp. 2387-2396, 2018.
- [45] F. Maier, J. Ristein and L. Ley, "Electron affinity of plasma-hydrogenated and chemically oxidized diamond (100) surfaces," *Physical Review B*, vol. 61, no. 165411, p. 64, 2001.
- [46] S. Cui and E. L. Hu, "Increased negatively charged nitrogen-vacancy centers in fluorinated diamond," *Applied Physics Letters*, vol. 103, no. 5, p. 051603, 2013.
- [47] S. Petrick and C. Benndorf, "Potassium adsorption on hydrogen- and oxygen-terminated diamond (100) surfaces," *Diamond and related materials*, vol. 10, no. 3-7, pp. 519-525, 2001.
- [48] P. Baumann and R. Nemanich, "Surface cleaning, electronic states and electron affinity of diamond (100), (111), and (110) surfaces," *Surface Science*, vol. 409, no. 2, pp. 320-335, 1998.
- [49] M. Riedel, J. Ristein and L. Ley, "The impact of ozone on the surface conductivity of single crystal diamond," *Diamond and Related Materials*, vol. 13, no. 4-8, pp. 746-750, 2004.
- [50] J. I. Enriquez, F. Muttaquien, M. Michiuchi, K. Inagaki, M. Geshi, I. Hamada and Y. Morikawa, "Oxidative etching mechanism of the diamond (100) surface," *Carbon*, vol. 174, pp. 36-51, 2021.
- [51] P. John, N. Polwart, C. E. Troupe and J. I. Wilson, "The Oxidation of Diamond: The Geometry and Stretching Frequency of Carbonyl on the (100) Surface," *Journal of the American Chemical Society*, vol. 125, no. 22, pp. 6600-6601, 2003.
- [52] P. E. Pehrsson, T. W. Mercer and J. A. Chaney, "Thermal oxidation of the hydrogenated diamond (100) surface," *Surface science*, vol. 497, no. 1-3, pp. 13-28, 2002.
- [53] G. Speranza, S. Torrenzo, M. Filippi, L. Minati, E. Vittone, A. Pasquarelli, M. Dipalo and E. Kohn, "In situ thermal treatment of UV-oxidized diamond hydrogenated surface," *Surface Science*, vol. 604, no. 9-10, pp. 753-761, 2010.
- [54] S. Torregio, "Surface functionalization and characterization of diamond thin films for sensing applications," University of Trento, Trento, 2010.
- [55] V. Loktev, V. Makal'skii, I. Stoyanova, A. Kalinkin and V. Likhonobov, "Surface modification of ultradispersed diamonds," *Carbon*, vol. 29, no. 7, pp. 817-819, 1991.
- [56] N. Fairley, V. Fernandez, M. Richard-Plouet, C. Guillot-Deudon, J. Walton, E. Smith, D. Flahaut, M. Greiner, M. Biesinger, S. Tougaard, D. Morgan and J. Baltrusaitis, "Systematic

- and collaborative approach to problem solving using X-ray photoelectron spectroscopy," *Applied Surface Science Advances*, vol. 5, p. 100112, 2021.
- [57] T. R. Gengenbach, G. H. Major, M. R. Linford and C. D. Easton, "Practical guides for x-ray photoelectron spectroscopy (XPS): Interpreting the carbon 1s spectrum," *Journal of Vacuum Science & Technology A*, vol. 39, no. 1, p. 013204, 2021.
- [58] P. Clews, G. Nelson, C. Matlock, P. Resnick and C. Adkins, "Minimizing sulfur contamination and rinse water volume required following a sulfuric acid/hydrogen peroxide clean by performing a chemically basic rinse," Sandia National Lab, Albuquerque, 1997.
- [59] P. Clews, G. Nelson, C. Matlock, P. Resnick, C. Adkins and N. Korbe, "Sulfuric acid/hydrogen peroxide rinsing study," Sandia National Laboratories, Albuquerque, 1995.
- [60] J. Liang, S. Masuya, M. Kasu and N. Shigekawa, "Realization of direct bonding of single crystal diamond and Si substrates," *Applied Physics Letters*, vol. 110, no. 11, p. 111603, 2017.
- [61] A. Dychalska, W. Koczorowski, M. Trzcinski, L. Mosinska and M. Szybowicz, "The Effect of Surface Treatment on Structural Properties of CVD Diamond Layers with Different Grain Sizes Studied by Raman Spectroscopy," *Materials*, vol. 14, no. 5, p. 1301, 2021.
- [62] K. Paprocki, A. Dittmar-Witsuki, M. Trzciński, M. Szybowicz, K. Fabisiak and A. Dychalska, "The comparative studies of HF CVD diamond films by Raman and XPS spectroscopies," *Optical Materials*, vol. 95, p. 109251, 2019.
- [63] V. Jain, M. C. Biesinger and M. R. Linford, "The Gaussian-Lorentzian Sum, Product, and Convolution (Voigt) functions in the context of peak fitting X-ray photoelectron spectroscopy (XPS) narrow scans," *Applied Surface Science*, vol. 447, pp. 548-553, 2018.
- [64] G. H. Major, V. Fernandez, N. Fairley, E. F. Smith and M. R. Linford, "Guide to XPS data analysis: Applying appropriate constraints to synthetic peaks in XPS peak fitting," *Journal of Vacuum Science & Technology A*, vol. 40, no. 6, p. 063201, 2022.
- [65] G. H. Major, T. G. Avval, B. Moeini, G. Pinto, D. Shah, V. Jain, V. Carver, W. Skinner, T. R. Gengenbach, C. D. Easton, A. Herrera-Gomez, T. S. Nunney, D. R. Baer and M. R. Linford, "Assessment of the frequency and nature of erroneous x-ray photoelectron spectroscopy analyses in the scientific literature," *Journal of Vacuum Science & Technology A*, vol. 38, no. 6, p. 061204, 2020.
- [66] P. M. Sherwood, "The use and misuse of curve fitting in the analysis of core X-ray photoelectron spectroscopic data," *Surface and Interface Analysis*, vol. 51, no. 6, pp. 589-610, 2019.
- [67] D. R. Baer, G. E. McGuire, K. Artyushkova, C. D. Easton, M. H. Engelhard and A. G. Shard, "Introduction to topical collection: Reproducibility challenges and solutions with a

focus on guides to XPS analysis," *Journal of Vacuum Science & Technology A: Vacuum, Surfaces, and Films*, vol. 39, no. 2, p. 021601, 2021.

- [68] T. Haensel, J. Uhlig, R. J. Koch, S. Imad-Uddin Ahmed, J. A. Garrido, D. Steinmuller-Nethl, M. Sutuzmann and J. A. Schaefer, "Influence of hydrogen on nanocrystalline diamond surfaces investigated with HREELS and XPS," *physica status solidi (a)*, vol. 206, no. 9, pp. 2022-2027, 2009.
- [69] K. Paprocki, A. Dittmar-Wituski, M. Trzcinski, M. Szybowicz, K. Fabisiak and A. Dychalska, "The comparative studies of HF CVD diamond films by Raman and XPS spectroscopies," *Optical Materials*, vol. 95, p. 109251, 2019.
- [70] R. Hoffman, A. Kriele, H. Obloh, J. Hees, M. Wolfer, W. Smirnov, N. Yang and C. E. Nebel, "Electrochemical hydrogen termination of boron-doped diamond," *Applied Physics Letters*, vol. 97, no. 5, p. 052103, 2010.
- [71] S. Ghodbane, D. Ballutaud, F. Omnes and C. Agnes, "Comparison of the XPS spectra from homoepitaxial {111},{100} and polycrystalline boron-doped diamond films," *Diamond and Related Materials*, vol. 19, no. 5-6, pp. 630-636, 2010.
- [72] S. Ghodbane, D. Ballutaud, A. Deneuve and C. Baron, "Influence of boron concentration on the XPS spectra of the (100) surface of homoepitaxial boron-doped diamond films," *physica status solidi*, vol. 203, no. 12, pp. 3147-3151, 2006.
- [73] V. Seshan, D. Ullien, A. Castellanos-Gomez, S. Sachdeva, D. Murthy, T. Savenije, H. Ahmad, T. Nunnay, S. Janssens, K. Haenen, M. Nesladek, H. van der Zant, E. Sudholter and L. de Smet, "Hydrogen termination of CVD diamond films by high-temperature annealing at atmospheric pressure," *The Journal of chemical physics*, vol. 138, no. 23, p. 234707, 2013.
- [74] D. Ballutaud, N. Simon, H. Girard, E. Rzepka and B. Bouchet-Fabre, "Photoelectron spectroscopy of hydrogen at the polycrystalline diamond surface," *Diamond and related materials*, vol. 15, no. 4-8, pp. 716-719, 2006.

Supplementary Information for “Effects of molecular contamination and sp<sup>2</sup> carbon on oxidation of (100) single-crystal diamond surface”

Ricardo Vidrio<sup>1,8,\*</sup>, Daniel Vincent<sup>2,8</sup>, Benjamin Bachman<sup>4</sup>, Cesar Saucedo<sup>4</sup>, Maryam Zahedian<sup>1</sup>, Zihong Xu<sup>1</sup>, Junyu Lai<sup>7</sup>, Timothy A. Grotjohn<sup>5</sup>, Shimon Kolkowitz<sup>6</sup>, Jung-Hun Seo<sup>7</sup>, Robert J. Hamers<sup>4</sup>, Keith G. Ray<sup>3</sup>, Zhenqiang Ma<sup>2</sup>, Jennifer T. Choy<sup>1,2,\*</sup>

<sup>1</sup>1500 Engineering Dr, Madison WI 53706, Department of Nuclear Engineering and Engineering Physics, University of Wisconsin-Madison

<sup>2</sup>1415 Engineering Dr, Madison WI 53706, Department of Electrical and Computer Engineering, University of Wisconsin-Madison

<sup>3</sup>7000 East Ave, Livermore CA 94550, Lawrence Livermore National Laboratory

<sup>4</sup>1101 University Ave, Madison WI 53706, Department of Chemistry, University of Wisconsin-Madison

<sup>5</sup>428 S Shaw Ln, East Lansing MI 48824, Electrical and Computer Engineering, Michigan State University

<sup>6</sup>1150 University Ave, Madison WI 53706, Department of Physics, University of Wisconsin-Madison

<sup>7</sup>135 Bell Hall, Buffalo NY 14260, Department of Materials Design and Innovation, University at Buffalo

<sup>8</sup>These authors contributed equally to this work.

The following section details the peak area percentages for each C1s fit performed on all wet chemistry oxidation samples. Samples that have been super-polished have been labeled as (SP).

*Table 1: Peak areas and counts for all identified functional groups of C1s peak deconvolution for all O-terminated diamond samples*

Treatment	sp <sup>3</sup> C Area (%)	sp <sup>3</sup> C Area (Counts)	sp <sup>2</sup> C Area (%)	sp <sup>2</sup> C Area (Counts)	C-O Area (%)	C-O Area (Counts)	C=O Area (%)	C=O Area (Counts)
Tri-Acid Clean #1	74.02 ± 0.29	20375.8 ± 79.83	14.65 ± 0.21	4030.16 ± 57.77	8.46 ± 0.29	2328.03 ± 79.80	2.88 ± 0.21	791.93 ± 57.74
Tri-Acid Clean #2	77.33 ± 0.28	21196.8 ± 76.75	13.26 ± 0.20	3635.45 ± 54.83	7.27 ± 0.30	1993.94 ± 82.28	2.14 ± 0.18	586.23 ± 49.31
Tri-Acid Clean #3	75.44 ± 0.29	21638.3 ± 83.18	13.75 ± 0.17	3944.0 ± 48.76	9.12 ± 0.29	2617.40 ± 83.23	1.68 ± 0.29	483.20 ± 83.41
Tri-Acid Clean #4	74.94 ± 0.32	21547.9 ± 92.01	13.40 ± 0.24	3851.86 ± 68.99	9.58 ± 0.25	2755.53 ± 71.91	2.08 ± 0.19	597.64 ± 54.59
Tri-Acid Clean #5	74.66 ± 0.26	20328.8 ± 70.79	12.32 ± 0.31	3353.72 ± 84.39	11.1 ± 0.39	3034.21 ± 106.22	1.88 ± 0.19	511.10 ± 51.65

\*Corresponding authors: [jennifer.choy@wisc.edu](mailto:jennifer.choy@wisc.edu) (Jennifer Choy)  
[vidrio@wisc.edu](mailto:vidrio@wisc.edu) (Ricardo Vidrio)

## Supplementary Information

Tri-Acid Clean #6	76.01 ± 0.28	19512.4 0 ± 71.88	13.50 ± 0.24	3466.35 ± 61.62	8.43 ± 0.27	2164.67 ± 69.33	2.06 ± 0.16	528.78 ± 41.07
H2SO4:HNO 3 #1	75.68 ± 0.24	21670.1 8 ± 68.72	13.86 ± 0.19	3968.72 ± 54.41	8.18 ± 0.34	2344.20 ± 97.44	2.27 ± 0.19	651.76 ± 54.55
H2SO4:HNO 3 #2	75.19 ± 0.30	21125.4 5 ± 84.29	14.17 ± 0.24	3980.10 ± 67.41	8.76 ± 0.39	2461.00 ± 109.57	1.89 ± 0.19	530.66 ± 53.35
Piranha Clean #1	76.01 ± 0.24	22336.8 9 ± 70.53	13.18 ± 0.22	3870.95 ± 64.61	8.98 ± 0.32	2638.98 ± 94.04	1.84 ± 0.14	540.83 ± 41.15
Piranha Clean #2	74.05 ± 0.31	21422.2 5 ± 89.68	12.96 ± 0.17	3747.62 ± 49.16	10.9 5 ± 0.37	3168.50 ± 107.06	2.04 ± 0.19	590.91 ± 55.04
ALD Water Vapor 15 Cycles	76.84 ± 0.31	22852.9 9 ± 92.20	11.20 ± 0.22	3329.59 ± 65.40	9.89 ± 0.27	2942.52 ± 80.33	2.07 ± 0.16	614.72 ± 47.51
ALD Water Vapor 30 Cycles	76.36 ± 0.32	20615.8 1 ± 86.39	11.58 ± 0.28	3125.07 ± 75.56	9.72 ± 0.36	2623.35 ± 97.16	2.35 ± 0.25	634.75 ± 67.53
UV/Ozone #1	74.44 ± 0.36	19582.2 4 ± 94.70	12.74 ± 0.30	3350.17 ± 78.89	9.77 ± 0.35	2570.03 ± 92.07	3.05 ± 0.18	803.36 ± 47.41
UV/Ozone #2	75.59 ± 0.35	21545.0 3 ± 99.76	12.17 ± 0.25	3467.77 ± 71.24	9.38 ± 0.29	2673.43 ± 82.65	2.86 ± 0.19	814.94 ± 54.14
ALD Water Vapor 15 Cycles (SP)	75.44 ± 0.29	30923.7 1 ± 118.87	15.68 ± 0.19	6426.02 ± 77.87	6.74 ± 0.16	2762.18 ± 65.57	2.14 ± 0.18	877.73 ± 73.83
ALD Water Vapor 30 Cycles (SP)	77.35 ± 0.29	30303.6 9 ± 113.61	14.40 ± 0.22	5642.02 ± 86.20	6.13 ± 0.18	2403.24 ± 70.57	2.11 ± 0.19	827.22 ± 74.49
UV/Ozone (SP)	74.32 ± 0.25	29510.7 0 ± 99.27	15.47 ± 0.19	6140.36 ± 75.41	6.54 ± 0.24	2595.44 ± 95.24	3.68 ± 0.17	1460.26 ± 67.46
Tri-Acid Clean (SP)	77.08 ± 0.40	32586.5 7 ± 169.11	12.50 ± 0.17	5285.08 ± 71.88	7.89 ± 0.40	3334.92 ± 169.07	2.53 ± 0.15	1071.50 ± 63.53

## Supplementary Information

The table below provides the binding energy peak position average and error for all oxidized diamond samples.

*Table 2: Binding energy peak positions for all identified functional groups for all O-terminated diamond samples*

Chemical Bond	Peak Position Average (eV)	Peak Position Error (eV)
sp <sup>3</sup> C	285.22	0.41
sp <sup>2</sup> C	284.02	0.31
C=O	287.78	0.43
C-O	286.23	0.45

The table below lists the peak area percentages for each C1s fit performed on the hydrogen terminated samples only.

*Table 3: Peak area information for all identified functional groups from C1s peak deconvolution of H-terminated data*

Treatment	Sp <sup>3</sup> Area (%)	Sp <sup>3</sup> Area (counts)	Sp <sup>2</sup> Area (%)	Sp <sup>2</sup> Area (counts)	C-H Area (%)	C-H Area (counts)	C-O Area (%)	C-O Area (counts)
H-Term #1	76.45 ± 0.31	21032.13 ± 85.28	6.40 ± 0.23	1760.25 ± 63.26	15.57 ± 0.33	4285.46 ± 90.83	1.58 ± 0.26	435.51 ± 71.67
H-Term #2	79.00 ± 0.35	20803.53 ± 92.17	5.05 ± 0.25	1328.82 ± 65.78	14.80 ± 0.34	3898.57 ± 89.56	1.15 ± 0.24	303.58 ± 63.36

## Supplementary Information

The table below lists the H-terminated sample followed by a subsequent acid exposure. The samples that followed the original procedure as Wang et. al are shown as “HC” and the samples that had the modified procedure with the tri-acid clean are termed as “HTC”.

*Table 4: Peak area information for all C1s peak deconvolution for H-terminated plus oxidation treated diamond samples*

Bonding Type	HC
Sp3 Area (%)	70.91 ± 0.98
Sp3 Area (counts)	19257.12 ± 266.14
Sp2 Area (%)	3.83 ± 0.48
Sp2 Area (counts)	1038.84 ± 130.19
C-H Area (%)	21.39 ± 0.67
C-H Area (counts)	5808.39 ± 181.94
C-O Area (%)	2.90 ± 0.32
C-O Area (counts)	788.52 ± 87.01
C=O Area (%)	0.98 ± 0.16
C=O Area (counts)	265.85 ± 43.40



## Supplementary Information

The two tables below lists the binding energy peak position values for all hydrogen treated samples. Table 6 has only the H-terminated data, while Table 7 has the H-terminated plus subsequent acid treatment data. The tables have been separated out this way as the change in the electron affinity values on the surface have altered the relative peak positions.

*Table 5: Binding energy peak positions for all identified functional groups from H-terminated diamond samples*

Chemical Bond	Peak Position Average (eV)	Peak Position Error (eV)
sp3 C	282.77	1.83E-2
sp2 C	282.04	7.07E-2
C-H	283.44	7.78E-2
C-O	285	1.41E-2

*Table 6: Binding energy peak positions for all identified functional groups from H-terminated plus oxidized diamond samples*

Chemical Bond	Peak Position (eV)
sp3 C	284.03
sp2 C	283.23
C-H	284.20
C-O	285.78
C=O	287.09